Cooperative Synthesis of Control and Display Augmentation

Sanjay Garg* and D. K. Schmidt†
Purdue University, West Lafayette, Indiana

The cooperative control synthesis technique, previously developed to synthesize control augmentation so as to optimize the human operator's subjective rating, is extended to the synthesis of display augmentation for closed-loop manual control tasks. The procedure allows for simultaneously augmenting the display dynamics as well as plant or controlled element dynamics via feedback, and explicitly includes task-related and pilot-centered requirements in the design objectives. Connections are made between the proposed technique and classical manual control theory, and the new methodology is demonstrated by considering a compensatory tracking task for a generic controlled element. Analytical evaluations of the various control and display augmentation results and comparisons with the results of previous experimental studies are discussed.

Introduction

THE amount of information to be processed by the pilot of a modern aircraft to accomplish an assigned task successfully has continued to increase. It is therefore becoming more and more critical to determine the best information set and display dynamics needed by the pilot so as to reduce the workload and improve performance.

In Ref. 1 it was hypothesized that a tradeoff exists between levels of control augmentation of a plant and display augmentation, in terms of workload and task performance. That is, a highly sophisticated display with minimum stability augmentation or a high level of control augmentation with lesser display integration, or intermediate combinations thereof, may lead to acceptable task performance and workload. The hypothesis of Ref. 1 was borne out by the extensive work done by Lebacqz et al.[2] and Lebacqz[3] in their effort to quantify the display/control requirements for helicopter approach and landing. They report that "the hypothesized tradeoff between display sophistication and control complexity was evident for combinations rated satisfactory, but the determination of an adequate combination is dependent primarily on stability-control augmentation."[2] Even with flight directors for all three axes, the pilots found it difficult to fly without adequate flight control augmentation.

Another area where display/control tradeoffs may be of importance is remotely piloted vehicles. A very high degree of accuracy in following complex trajectories can be achieved by completely automatic controllers,[4] but it may be undesirable to take the human controller completely out of the control loop for reasons of safety or mission flexibility. A combination of "intelligent" remote displays[5] and control augmentation of the vehicle may then lead to desirable levels of accuracy while still maintaining manual control.

Thus, there exists a need to synthesize stability augmentation and display augmentation with special attention to the role of the human in the system. The idea that a control augmentation system works in cooperation with the human, and that a technique which considers the augmentation system and the human to be two controllers working in "parallel" was suggested by Schmidt.[6] This cooperative control synthesis technique (CCS) incorporates a mathematical model of the manual control behavior, and uses optimal-control theory to synthesize feedback control gains such that the augmented plant dynamics are "pilot-optimal." Because display augmentation, like control augmentation, has to be in harmony with the human's abilities and limitations, the cooperative synthesis technique was considered to provide an appropriate framework for simultaneously synthesizing control *and* display augmentation, and thus provides a task-specific tradeoff between such control and display augmentation systems.

Other display design techniques based on an optimal control model (OCM)[7] of manual control behavior have been suggested by Levison,[8] Hess,[9] and Hoffman et al.[10] All these techniques are intended to lead to flight director designs that reduce pilot workload, and are clever applications of the OCM. An excellent discussion of the functional requirements for the design of flight directors can also be found in Ref. 11. The fundamental control and guidance requirement stated is to reduce the tracking error to zero in a stable, well damped, and rapid manner. Based on the crossover model of the human pilot,[12] the main pilot-centered requirement, whether considering control or display augmentation, is that the effective controlled element as perceived by the pilot is like k/s over a broad frequency region. With such a controlled element, the pilot's compensation is reduced to that of a pure gain in the crossover region, which is considered optimal from the point of minimum pilot workload. All of the preceding techniques involve designing the flight director control law for a given plant or controlled element. Therefore, these methods do not explicitly include the display/control tradeoff in the synthesis procedures themselves. Furthermore, not only must the pilot-centered requirements be met, but good overall closed-loop performance also must be obtained. As will be shown, a performance/workload tradeoff exists.

This paper presents a methodology intended to provide a systematic approach to synthesizing pilot-optimal control and display augmentation in complex closed-loop manual control tasks. This methodology is an extension of the cooperative control synthesis technique developed earlier[6,13] for control augmentation synthesis. The characteristic results from the methodology are evaluated by considering a compensatory tracking task with a simple, but difficult to control, plant. Although the methodology is clearly intended for higher order multichannel tasks, use of this plant and task is appropriate to gain insight, and for validation studies. With such a plant, the crossover model[12] can be used effectively to gain such insight, and to compare results with those obtained from the cooperative synthesis approach.

Presented as Paper 86-2204 at the AIAA 1986 Guidance, Navigation, and Control Conference, Williamsburg, VA, Aug. 18-20, 1986; received Jan. 26, 1987; revision received July 4, 1987.

*Ph.D. Candidate. Member AIAA.

†Professor, School of Aeronautics and Astronautics; currently, Controls Engineer, Lewis Research Group, Sverdrup Technology, Middleburg Heights, OH. Associate Fellow AIAA.

Preliminary Analysis

Consider a compensatory tracking task with a K_o/s^2 plant, as in Fig. 1. As is well known, such a plant is difficult to control in that it requires the human to generate a significant amount of lead, which results in deterioration in performance and subjective ratings. Now, rate feedback can be used to provide lead, either in the form of a "quickened" display, or through augmenting the plant dynamics using feedback, or a combination of both, as shown in Fig. 2. In Fig. 2, K_d is the display "quickening" gain and K_c is the plant augmentation feedback control gain. A feedforward gain K_δ on the manual control input (δ_p) is used to compensate for the reduced static gain of the plant when using the feedback control augmentation shown.

With display augmentation only [i.e., $D(s) = 1$, $K_\delta = K_c = 0$ in Fig. 2], the controlled element as seen by the human is

$$x_d(s)/\delta_p(s) = \frac{K_o(K_d s + 1)}{s^2}$$

Thus this effective controlled element is like k/s for frequencies greater than $1/K_d$. Extensive experimental work, by McRuer and Jex,[12] has shown that for a pure k/s element, the crossover frequency of the manually controlled system is $\omega_c \approx 4.3$ rads/s, and the pilot's compensation in the crossover region is given by $P(s) = K_p e^{-\tau s}$, with $\tau \approx 0.23$ s for a command input bandwidth of 1.5 rad/s. Without any pilot lead compensation, which is undesirable from pilot workload considerations, the minimum value of K_d just to stabilize the loop, with the above form of $P(s)$, is 0.36 for $\omega_c = 4.3$ rads/s.

The true tracking error $e(s)$ is given by

$$e(s)/\theta_c(s) = \frac{s[s + K_o K_d P(s)]}{[s^2 + K_o K_d P(s)s + K_o P(s)]}$$

Thus, for a step command, the steady-state error approaches zero, which shows that this rate-augmented display satisfies the control and guidance requirement of Ref. 11. However, the loop transfer function with the loop broken at the perceived signal x_d (see Fig. 2, with $K_\delta = K_c = 0$) is given by

$$P(s)\frac{K_o}{s^2}(1 + K_d s) \tag{1}$$

while the loop transfer function with the loop broken at the true error e is given by

$$P(s)\frac{K_o}{s^2}\left(\frac{s}{s + P(s)K_o K_d}\right) \tag{2}$$

From these two expressions it can be inferred that the crossover frequency for the x_d loop [Eq. (1)] will be greater than that for the error loop [Eq. (2)]. This implies that the error perceived by the human (x_d) will always be less than the actual error, and the difference will increase as K_d is increased. Thus, though a high value of K_d may be desirable from the point of reduced operator workload, making K_d too high will actually result in tracking performance deterioration.

Conversely, consider control augmentation without an augmented display [i.e., Fig. 2 with $D(s) = 1$, $K_d = 0$]. Now, with rate feedback augmenting the plant, the effective and true controlled element are the same, and given by

$$\theta(s)/\delta_p(s) = \frac{K_o K_c}{s(s + K_o K_c)}$$

(Here, $1 + K_\delta \approx K_c$ is assumed.) Thus the controlled element is like k/s for frequencies less than $K_o K_c$. Using the previous argument, for the system to be just stable with no pilot lead compensation (i.e., $P(s) = K_p e^{-0.23s}$) requires a minimum value of 7.8 for $K_o K_c$, if $\omega_c \approx 4.3$ rad/s. Increasing K_c above this minimum reduces phase lead required of the pilot to provide adequate phase margins, or pilot workload is minimized. Because the displayed error and perceived error are the same (in contrast to the previous case), there is no performance decrement as K_c is increased. However, there would be restrictions on the gain based on other requirements, such as limits, for example, on loop bandwidth of the control-augmented system.

Even though the objective of both the control augmentation and display augmentation is to reduce the required manual control compensation, the way this is achieved is fundamentally different. In display augmentation, the required lead is provided through a change in the numerator dynamics of the effective controlled element, while in control augmentation the controlled plant poles are changed, thus affecting the stability properties of the controlled element.

Now, with both control and display augmentation, the effective controlled element is

$$x_d(s)/\delta_p(s) = \frac{K_o K_c(K_d s + 1)}{s(s + K_o K_c)} \tag{3}$$

Clearly, by letting $K_o K_c = 1/K_d$, the controlled element can be made exactly k/s. But, as stated earlier, there would be limits imposed on values of K_c and K_d by requirements other than those of just minimizing pilot workload. And, although the compensation required of the human for any such combination of K_d and $K_o K_c$ is the same, the actual tracking error and the augmented plant bandwidth do vary. Consequently, even in this simple example, one is already faced with the question of how to "best" tradeoff control and display augmentation.

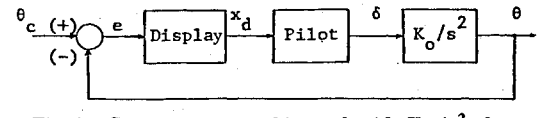

Fig. 1 Compensatory tracking task with K_o/s^2 plant.

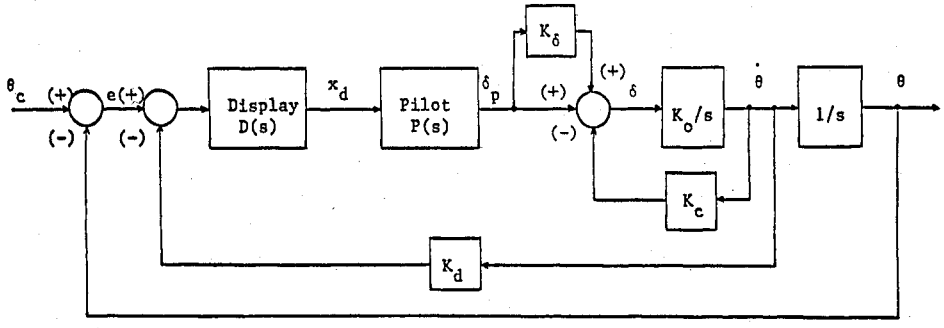

Fig. 2 Display / control augmentation using rate feedback.

Application of Cooperative Synthesis

In the Appendix, a mathematical optimization problem is discussed and the necessary conditions for optimality are derived. The interaction between the various controllers is shown in Fig. A1. The association of controller $\bar{u}_a$ with plant augmentation and of display control $\bar{u}_d$ with the display augmentation should be apparent in this formulation. Moreover, with $\bar{u}_p \triangleq \dot{\bar{\delta}}_p$ ($\bar{\delta}_p$, the manual control input), along with appropriate definition of the system matrices A_o and B_{1o}, the structure of the controller $\bar{u}_p$ that evolves from the above formulation is similar to that of an OCM of manual control.[7] The elimination of the human operator's time delay in the synthesis model simplifies the dynamic order by eliminating the linear predictor present in the complete OCM control structure. The motor noise $\bar{v}_m$ is, however, accounted for in this formulation in that it may appear as an additional disturbance in Eq. (A1).

Though the simplified model is used in the synthesis procedure, a complete model (with predictor, etc,) is used to evaluate candidate designs. Moreover, at each iteration of the synthesis process, the parameters (e.g., noise intensities) in the simplified model are updated to yield results that are consistent with the complete OCM model. It has been shown[14] that by selecting proper noise intensities for the motor noise $\bar{v}_m$ and the measurement noise $\bar{v}_y$, the simplified model yields the same human operator dynamics as the complete model.

Consider again the simple compensatory tracking task as in Fig. 1 and in Ref. 6. Let the command signal θ_c be filtered white noise w, with

$$\theta_c(s)/w(s) = 3.67/(s^2 + 3s + 2.25)$$

and

$$E(w) = 0 \qquad E\{w(t)w(t+\sigma)\} = \delta(\sigma)$$

It is assumed that the error signal is displayed to the human with $D(s)$ consisting of a first order lag at 50 rad/s, or

$$x_d(s) = \frac{50}{(s+50)} e(s)$$

The human's observations are the displayed variable x_d (and its associated rate $\dot{x}_d$, as per the OCM) and his objective is to regulate the displayed signal. This task is interpreted as that of minimizing the performance index

$$J_p = E\left\{ \lim_{T\to\infty} \frac{1}{T} \int_o^T \left(x_d^2 + g_p \dot{\delta}_p^2 \right) \mathrm{d}t \right\} \tag{4}$$

where g_p may be chosen to yield a particular neuromuscular lag time constant, for example, $\tau_n = 0.1$ s.

For all the results presented here, the following were assumed in the OCM evaluation of the task, and these are all consistent with the standard modeling assumptions in Ref. 7:

1) The human is assumed to reconstruct the rate information $\dot{x}_d$ from the displayed variable x_d.

2) Observation thresholds for x_d and $\dot{x}_d$ are 0.012 in. and 0.036 in./s, respectively, based on visual arc angles of 0.05 deg and 0.15 deg/s at the human controller's eye, and assuming the display to be 1 ft away.

3) The observation noise ratio is -20 dB for each observation (x_d and $\dot{x}_d$).

4) The motor noise ratio is -20 dB.

5) The observation time delay is $\tau = 0.1$ s.

The predicted manually controlled system performance for the unaugmented plant is given in Table 1. (Note that the statistical results differ from those in Ref. 6 because of the different observation thresholds for the display considered.) The frequency domain results are presented and discussed later in this paper.

The results in Table 1 are indicative of high levels of tracking error and workload, which may be reduced by a suitable choice of display or control augmentation using only $\dot{\theta}$ feedback, again, as shown in Fig. 2 and consistent with the previous discussion. Within the framework of the cooperative synthesis methodology presented in the Appendix, the augmentation shown in Fig. 2 leads to the following definitions:

$$\bar{y}_p = [x_d, \dot{x}_d]^T + \bar{v}_y, \quad \bar{y}_a = \left[\dot{\theta}, \delta_p\right]^T, \quad y_d = \dot{\theta}$$

$$G_a = [-K_c, K_\delta], \quad G_d = -K_d, \quad J_1 = J_p$$

[with J_p as in Eq. (4)]

The choice of the synthesis cost function J_2 should reflect the various tradeoffs that are involved. For the results presented herein, J_2 was chosen to be

$$J_2 = E\left\{ \lim_{T\to\infty} \frac{1}{T} \int_o^T \left(e^2 + g_p \dot{\delta}_p^2 + F_2 u_a^2 + F_{2d} u_d^2 \right) \mathrm{d}t \right\}$$

with $g_p = 0.009$ (corresponding to g_p for the unaugmented case, as in Table 1.). Wierwille and Connor[15] have shown that the human's perception of manual control workload is strongly correlated with the rms value of his control input rate, so the inclusion of $\dot{\delta}_p$ in the cost function J_2 reflects the desire to minimize this workload. Clearly the inclusion of error reflects the desire to provide good tracking performance. (Note that J_p is different from J_2 in that J_p consists of minimizing x_d, the displayed signal being observed by the pilot, while J_2 consists of minimizing the actual tracking error which is the ultimate task objective.) The weights F_2 and F_{2d} (scalars for this case) are design variables, chosen to adjust the levels of augmentation control energy and "display energy," respectively. For $F_2 = F_{2d} = 0$ and $x_d = e$, $J_2 = J_p$.

Using this cooperative methodology, four different cases of augmentation were considered. These cases are discussed below.

Display Augmentation Only

The results for display augmentation only (i.e., $F_2 = \infty$), for varying F_{2d}, are listed in Table 2 along with the evaluation results using the full-order OCM model. As expected, the value of K_d tends to increase as weighting F_{2d} is decreased. But, interestingly, K_d reaches a limiting value of 0.373 in./deg-s^{-1} as $F_{2d} \to 0$. Thus, as the allowable value of display gain is increased, the methodology leads to a design that meets the pilot-centered requirements of Ref. 11. Note that the limiting value of K_d is very close to the value of K_d obtained earlier ($K_d \approx 0.36$) using the crossover model.

The results of Table 2 are also plotted in Fig. 3. It is clear from this figure that the pilot's workload (as measured by rms $\dot{\delta}_p$) decreases monotonically as the display augmentation gain K_d is increased. Conversely, the true rms error e initially

Table 1 Unaugmented system performance

g_p	e rms, deg	δ rms, deg	$\dot{\delta}_p$ rms, deg/s	J_p
0.009	0.812	0.802	5.95	0.98

Table 2 Display augmented system

F_{2d}	K_d	e rms, deg	δ rms, deg	$\dot{\delta}_p$ rms, deg/s	J_p
10	0.032	0.756	0.749	5.58	0.82
1	0.230	0.623	0.453	3.38	0.41
0.1	0.353	0.634	0.345	2.56	0.35
0.01	0.373	0.638	0.333	2.46	0.34
0.001	0.373	0.638	0.333	2.46	0.34

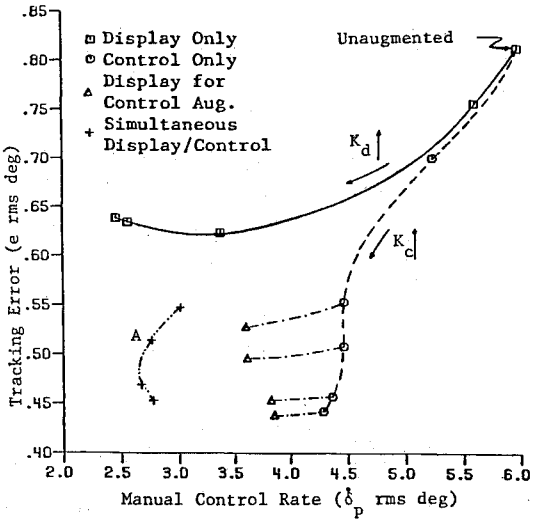

Fig. 3 Performance and workload comparison.

Table 3 Control augmented system

F_2	K_c, deg/deg-s^{-1}	K_δ	e rms, deg	δ rms, deg	$\dot{\delta}_p$ rms, deg/s	J_p
10	0.029	0.020	0.700	0.704	5.22	0.70
2	0.116	0.149	0.553	0.622	4.46	0.42
1	0.203	0.285	0.508	0.637	4.46	0.35
0.33	0.461	0.841	0.457	0.716	4.36	0.28
0.1	0.617	1.276	0.442	0.774	4.28	0.26
0.01	0.620	1.284	0.442	0.774	4.28	0.26

Table 4 Display design for control-augmented plants ($F_{2d} = 1$)

K_c deg/deg-s^{-1}	K_δ	K_d in./deg-s^{-1}	e rms, deg	δ rms, deg	$\dot{\delta}_p$ rms, deg/s	J_p
0.116	0.149	0.123	0.528	0.507	3.61	0.28
0.203	0.285	0.116	0.496	0.525	3.62	0.24
0.461	0.841	0.095	0.454	0.629	3.83	0.21
0.617	1.276	0.087	0.439	0.693	3.86	0.20

decreases as K_d is increased, but then increases. The limiting value of K_d ($= 0.373$) corresponds to that value beyond which increasing K_d will lead to degraded performance, without any significant reduction in workload. If the human operator's performance index J_p is used to predict the subjective opinion rating,[9,16] then the results in Table 2 also indicate that there will be no further improvement in opinion rating if K_d is increased beyond the limiting value.

Control Augmentation Only

The results for just control augmentation (i.e., $F_{2d} = \infty$) are listed in Table 3, along with the model-based results using the full-order OCM. Again, it is noted that as $F_2 \to 0$, a limiting value of $K_c \approx 0.62$ deg/deg-s^{-1} is achieved. This corresponds to $K_o K_c = 7.2$, quite close to the value 7.8 obtained earlier using the crossover model. Thus, as the allowable level of control energy is increased, the methodology leads to a design that again meets the pilot-centered requirements of Ref. 11. The results of Table 3 are also plotted in Fig. 3, indicating that the tracking performance (e) improves monotonically as the level of control augmentation is increased, and the workload ($\dot{\delta}_p$) also is reduced. But, as stated earlier, a high value of K_c may be undesirable. Therefore, an intermediate value may be chosen beyond which negligible improvement in tracking performance results, along with no noticeable reduction in operator workload ($\dot{\delta}_p$).

Comparing the results for display augmentation alone with those for control augmentation alone, it is evident that control augmentation has the advantage of significantly improving tracking performance with limited improvement in workload, while display augmentation can significantly reduce workload with limited improvement in actual tracking error. This again supports the conjecture that even for the simple k/s^2 plant, there appears to be some advantage in providing a combination of control and display augmentation, as opposed to only one or the other.

Table 5 Simultaneous display/control design ($F_{2d} = 1$)

F_2	K_c, deg/deg-s^{-1}	K_δ	K_d, in./deg-s^{-1}	e rms, deg	δ rms, deg	$\dot{\delta}_p$ rms, deg/s	J_p
2	0.082	0.260	0.153	0.547	0.479	3.02	0.29
1[a]	0.144	0.498	0.132	0.514	0.490	2.76	0.26
0.33	0.344	1.198	0.108	0.469	0.578	2.67	0.22
0.1	0.437	1.576	0.076	0.453	0.647	2.77	0.22

[a]Candidate design.

Display Design for Augmented Plants

For four rate-augmented plants, a separate display-augmentation synthesis was carried out, using the same cost index J_2 as before ($F_2 = \infty$, F_{2d} varied). As the level of display augmentation was increased (F_{2d} was decreased) for a given rate-augmented plant, the same trends were observed as in the case of display design for the unaugmented plant. That is, the actual error first decreases and then increases with increasing K_d, along with monotonic reduction in workload ($\dot{\delta}_p$). As in the case of a k/s^2 plant, the true tracking error was a minimum when $F_{2d} = 1$ for each of the four rate-augmented plants. The synthesis results and the predicted performance corresponding to the aforementioned weighting (i.e, $F_{2d} = 1$) are listed in Table 4. These results are also plotted in Fig. 3.

It is interesting to note from Table 4 that as the plant becomes more and more like k/s (or as K_c is increased), the optimum display augmentation gain decreases, even though the performance index being minimized (J_2) is the same in all cases. Also, the synthesized display augmentation is such that the pilot workload ($\dot{\delta}_p$) is roughly the same for all the cases presented in Table 4. This result is related to the findings in Ref. 2, that the workload can be constant over specific combinations of control and display sophistication.

Simultaneous Control/Display Synthesis

Finally, the cooperative synthesis algorithm was again exercised, except the control and display augmentation gains K_c and K_d were simultaneously obtained. The synthesis results and the predicted closed-loop performance are listed in Table 5, and plotted in Fig. 3. Again, as the level of control augmentation is increased ($F_2 \to 0$), the optimum display gain decreases. Comparing these results to those obtained in the section above, we note almost equal closed-loop performance (rms error), but the pilot's control input rate ($\dot{\delta}_p$) is much lower (25% less) in the case of simultaneous synthesis. This is true even when the results are compared for the same level of plant augmentation (K_c). This result is primarily caused by higher augmented plant sensitivities (higher values of K_δ) that are obtained when control/display gains are synthesized simultaneously, as compared to the case of synthesizing control augmentation only. The phenomenon that leads to this result is not completely understood at present and is the subject of ongoing research.

A hybrid design that offers improved performance and workload is the one obtained by simultaneous display/control synthesis and is indicated in Table 5. From Fig. 3 we note that for this case (labeled A in the figure), the tracking performance is much improved over the unaugmented case, the manual control input rate is much reduced, and the level of control augmentation (K_c) is modest. And, as Eq. (3) would indicate, the effective controlled element for the candidate design is close to k/s over a broad frequency region.

Table 6 Comparison between OCM and McDonnell[18] results

Controlled element	Classification	Results based on	ω_c, rad/s	ϕ_M, deg	τ_e s	T_L s	$\bar{x}_d^2/\bar{\theta}_c^2$
$\frac{K}{s^2}$	Unaugmented	OCM	3.1	26	0.36	1.2	0.66
		McDonnell[18]	2.9	20	0.33	>1	0.73
$\frac{K(0.37s+1)}{s^2}$	Display aug.	OCM	4.1	44	0.20	0.20	0.21
$\frac{K}{s(s+7.2)}$	Control aug.	OCM	3.7	53	0.17	0.19	0.20
$\frac{K}{s}$		McDonnell	4.0	40	0.20	0	0.18
$\frac{K(0.13s+1)}{s(s+1.68)}$	Candidate design	OCM	3.9	50	0.18	0.27	0.18

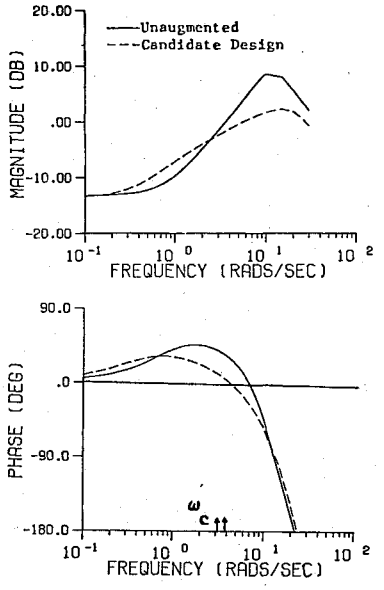

Fig. 4 Pilot describing function $[P(j\omega)]$.

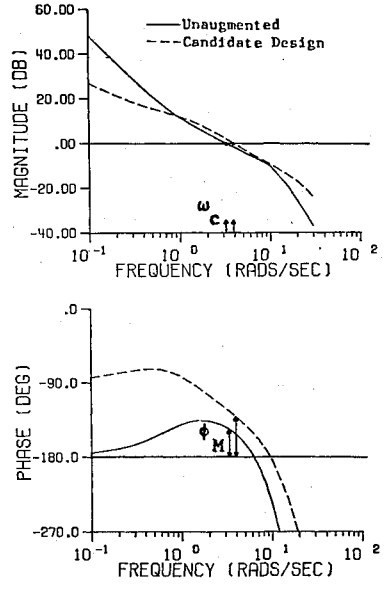

Fig. 5 Loop transfer function $[P(j\omega)] \cdot [x_d/\delta_p(j\omega)]$.

The manual controller describing function $[P(j\omega)]$, calculated from the OCM (see Ref. 17), for the above candidate design and the unaugmented plant are compared in Fig. 4, while the resulting loop frequency responses $[P(j\omega)] \cdot [x_d/\delta_p(j\omega)]$ are shown in Fig. 5. These figures indicate that, for the candidate design, not only is the manual controller's $[P(j\omega)]$ phase compensation reduced, as compared to that for the k/s^2 plant, but the loop crossover frequency is also higher, and the stability margins are much improved.

The model-based results may also be compared with those obtained in McDonnell's[18] experiments. Shown in Table 6 are the loop crossover frequency (ω_c), the phase margin (ϕ_M), the total effective time delay of the human operator (τ_e), the human's lead time constant (T_L), and the ratio of the mean-square perceived error to mean-square command input ($\bar{x}_d^2/\bar{\theta}_c^2$). Here, τ_e is obtained from the relation

$$\tau_e = \frac{(90 - \phi_M)}{\omega_c} \frac{\pi}{180}$$

where ϕ_M is in deg and is obtained from the loop Bode plots, as in Fig. 5. The human operator's phase compensation at crossover, as in Ref. 17, is used to calculate the lead time constant (T_L).

The model-based results for the unaugmented plant are in agreement with those of McDonnell. The OCM predictions for the best display-augmentation case and the best control-augmentation case ("best" in terms of minimum pilot workload) are also comparable with those obtained by McDonnell for a k/s controlled element. As the results for the hybrid design are also very close to the measured quantities for a k/s plant, this case should elicit an excellent subjective rating. McDonnell's results show a rating (based on the Cooper scale[19]) of 7 for the k/s^2 plant and 3 for the k/s plant. Based on correlations between pilot rating and various measured parameters such as T_L, τ_e, ω_c, and perceived performance, as found by McDonnell, all the synthesized designs listed in Table 6 then correspond to an improvement in subjective rating of about four on the Cooper scale. Thus, all these augmented systems would be rated "good".

Conclusions

An algorithmic methodology was presented that has the potential of providing a systematic tradeoff between control and display augmentation in manual control, taking into account the limitations of the human controller. Classical analysis of a k/s^2 plant was used to highlight what is meant by a control/display tradeoff. Various control and display augmentation laws were then synthesized using the algorithmic methodology, again with the same k/s^2 plant. Analytical evaluations of the synthesized results demonstrate the applicability of the methodology to meet the pilot-centered requirements for display design. The model-based results, when compared with previous experimental research, tend to validate the modeling procedure, thus enhancing the overall applicability of the methodology.

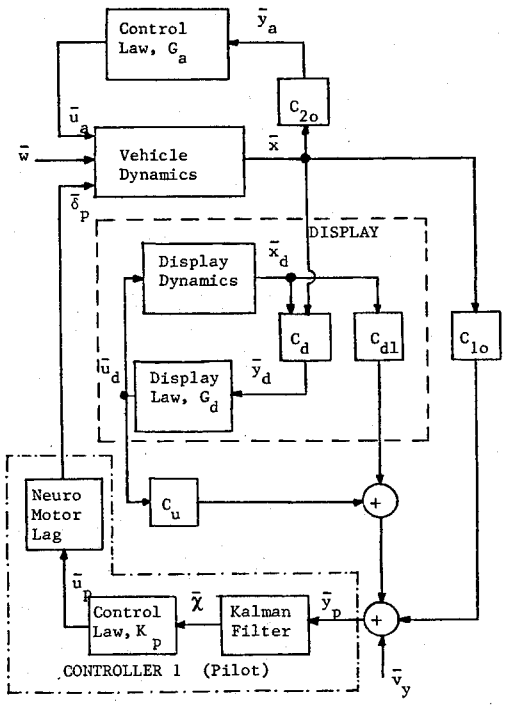

Fig. A1 Block diagram for cooperative control / display augmentation.

Appendix: Optimal Cooperative Control / Display Design Methodology

Problem Formulation

Consider a dynamic system acted upon by two physically independent controllers $\bar{u}_p$ and $\bar{u}_a$, and described by the linear time invariant set of first-order differential equations

$$\dot{\bar{x}} = A_o\bar{x} + B_{1o}\bar{u}_p + B_{2o}\bar{u}_a + D_o\bar{w} \tag{A1}$$

with $\bar{x} \in R^n$, $\bar{u}_p \in R^{m_1}$, $\bar{u}_a \in R^{m_2}$, and $\bar{w}$ a zero-mean Gaussian white noise process with intensity W. The controller $\bar{u}_p$ will correspond to the control input from the human pilot, while $\bar{u}_a$ is the control input from a feedback control law that will augment the plant dynamics.

The display dynamics that are present are assumed given in the form

$$\dot{\bar{x}}_d = A_d\bar{x}_d + B_{do}\bar{u}_d \tag{A2}$$

with $\bar{x}_d \in R^d$ and $\bar{u}_d \in R^{m_d}$, where $\bar{u}_d$ is the display "quickening" controller. The objective is to find the optimal cooperative controllers $\bar{u}_p$, $\bar{u}_a$, and $\bar{u}_d$.

Controller $\bar{u}_p$ is assumed to have noisy observations available for feedback given by

$$\bar{y}_p = C_{1o}\bar{x} + C_{1d}\bar{x}_d + C_u\bar{u}_d + \bar{v}_y \tag{A3}$$

where $\bar{v}_y$ is also a zero-mean Gaussian white noise process with intensity V_y. This controller will have the form of a linear quadratic Gaussian compensation, i.e., it consists of full-state feedback implemented using a Kalman estimator. As such, this controller can be made to closely approximate the optimal control model of manual control.[14]

The augmentation controller $\bar{u}_a$ and the display control law $\bar{u}_d$ are assumed to have noise-free measurements $\bar{y}_a$ and $\bar{y}_d$, respectively, available for feedback, where

$$\bar{y}_a = C_{2o}\bar{x}, \quad \bar{y}_d = C_d\begin{Bmatrix}\bar{x}\\ \bar{x}_d\end{Bmatrix} \tag{A4}$$

Note that the above formulation does not allow feedback of the display states $\bar{x}_d$ to the augmentation controller $\bar{u}_a$, although this could be added. Finally, these two latter controllers are constrained to have the direct output feedback form

$$\bar{u}_a = G_a\bar{y}_a = G_aC_{2o}\bar{x}$$

$$\bar{u}_d = G_d\bar{y}_d = G_dC_d\begin{Bmatrix}\bar{x}\\ \bar{x}_d\end{Bmatrix} \tag{A5}$$

Any dynamic compensation that may be desired (e.g., via state estimators) can be implemented based on the above form of the augmentation controllers ($\bar{u}_a$ and $\bar{u}_d$) with a proper definition of the states $\bar{x}$ and $\bar{x}_d$ and an appropriate choice of the outputs $\bar{y}_a$ and $\bar{y}_d$. These estimators can be determined after the gain synthesis presented here, in the standard manner.

The interaction between the different controllers is shown in the block diagram of Fig. A1.

Design Objectives

Controller 1 ($\bar{u}_p$) is to be optimal with respect to the cost

$$J_1 = E\left\{\lim_{T\to\infty}\frac{1}{T}\int_o^T\left(\bar{x}^TQ_{1o}\bar{x} + \bar{x}_d^TQ_{1d}\bar{x}_d + \bar{u}_p^TR_1\bar{u}_p + \bar{u}_a^TF_1\bar{u}_a\right)dt\right\} \tag{A6}$$

in the presence of the action of control inputs $\bar{u}_a$ and $\bar{u}_d$. Here $E\{\cdot\}$ indicates the expected value operator, and the weighting matrices are $Q_{1o} \geq 0$, $Q_{1d} \geq 0$, $R_1 > 0$, and $F_1 \geq 0$. Conversely, controller 2 ($\bar{u}_a$) and the display control law $\bar{u}_d$ are to be optimal with respect to the cost

$$J_2 = E\left\{\lim_{T\to\infty}\frac{1}{T}\int_o^T\left(\bar{x}^TQ_{2o}\bar{x} + \bar{x}_d^TQ_{2d}\bar{x}_d + \bar{u}_p^TR_2\bar{u}_p + \bar{u}_a^TF_2\bar{u}_a + \bar{u}_d^TF_{2d}\bar{u}_d\right)dt\right\} \tag{A7}$$

in the presence of the control action $\bar{u}_a$. The weighting matrices are $Q_{2o} \geq 0$, $Q_{2d} \geq 0$, $R_2 \geq 0$, $F_2 > 0$, and $F_{2d} > 0$.

Augmenting the system dynamics [Eq. (A1)] with the display dynamics [Eq. (A2)], the state-space description of this augmented system is

$$\begin{Bmatrix}\dot{\bar{x}}\\ \dot{\bar{x}}_d\end{Bmatrix} = \begin{bmatrix}A_o & 0\\ 0 & A_d\end{bmatrix}\begin{Bmatrix}\bar{x}\\ \bar{x}_d\end{Bmatrix} + \begin{bmatrix}B_{1o}\\ 0\end{bmatrix}\bar{u}_p + \begin{bmatrix}B_{2o}\\ 0\end{bmatrix}\bar{u}_a + \begin{bmatrix}0\\ B_{do}\end{bmatrix}\bar{u}_d + \begin{bmatrix}D_o\\ 0\end{bmatrix}\bar{w} \tag{A8}$$

Defining $\bar{\mathbf{x}} = \text{col}(\bar{x}, \bar{x}_d)$, Eq. (A8) can be written in a compact form with appropriate definitions for the matrices as

$$\dot{\bar{\mathbf{x}}} = A\bar{\mathbf{x}} + B_1\bar{u}_p + B_2\bar{u}_a + B_d\bar{u}_d + D\bar{w} \tag{A9}$$

The measurements can similarly be written as

$$\bar{y}_p = C_1\bar{\mathbf{x}} + C_u\bar{u}_d + \bar{v}_y$$

$$\bar{y}_a = C_2\bar{\mathbf{x}}$$

$$\bar{y}_d = C_d\bar{\mathbf{x}} \tag{A10}$$

The two cost functions can then be expressed in terms of the augmented state vector $\bar{\mathbf{x}}$ as

$$J_1 = E\left\{\lim_{T\to\infty}\frac{1}{T}\int_o^T\left(\bar{\mathbf{x}}^TQ_1\bar{\mathbf{x}} + \bar{u}_p^TR_1\bar{u}_p + \bar{u}_a^TF_1\bar{u}_a\right)dt\right\}$$

$$J_2 = E\left\{\lim_{T\to\infty}\frac{1}{T}\int_o^T\left(\bar{\mathbf{x}}^TQ_2\bar{\mathbf{x}} + \bar{u}_p^TR_2\bar{u}_p + \bar{u}_a^TF_2\bar{u}_a + \bar{u}_d^TF_{2d}\bar{u}_d\right)dt\right\} \tag{A11}$$

where the weighting matrices Q_1 and Q_2 are appropriately defined. Note that this formulation is formally that for a multiplayer nonzero sum game, and we seek a Nash solution.[20]

Solution for $\bar{u}_p$

In the presence of the action of control inputs $\bar{u}_a$ and $\bar{u}_d$, as given by Eq. (A5), the dynamics of the augmented system [Eq. (A9)] are

$$\dot{\bar{\chi}} = A_{\text{aug}}\bar{\chi} + B_1\bar{u}_p + D\bar{w}$$
$$\bar{y}_p = C_{\text{aug}}\bar{\chi} + \bar{v}_y \tag{A12}$$

where

$$A_{\text{aug}} \triangleq (A + B_2G_aC_2 + B_dG_dC_d)$$
$$C_{\text{aug}} \triangleq (C_1 + C_uG_dC_d) \tag{A13}$$

and the performance index J_1 becomes

$$J_1 = E\left\{ \lim_{T\to\infty} \frac{1}{T}\int_o^T \left[\bar{\chi}^T\left(Q_1 + C_2^TG_a^TF_1G_aC_2\right)\bar{\chi} + \bar{u}_p^TR_1\bar{u}_p\right] \mathrm{d}t \right\} \tag{A14}$$

Equations (A12) and (A14), in the case of uncorrelated process and measurement noises ($\bar{w}$ and $\bar{v}_y$) and for $V_y > 0$ (i.e., V_y positive definite), describe the standard nonsingular linear quadratic Gaussian regulator problem for controller $\bar{u}_p$. The optimal controller is known[21] to have the form

$$\bar{u}_p = K_p\hat{\bar{\chi}} \tag{A15}$$

where $\hat{\bar{\chi}}$ is the minimum mean-square estimate of the system state vector $\bar{\chi}$. The gain matrix K_p is given by

$$K_p = -R_1^{-1}B_1^TP \tag{A16}$$

with $P \geq 0$ and symmetric, the solution of the algebraic Ricatti equation

$$A_{\text{aug}}^TP + PA_{\text{aug}} + \left(Q_1 + C_2^TG_a^TF_1G_aC_2\right) - PB_1^TR_1^{-1}B_1P = 0 \tag{A17}$$

The dynamics of the Kalman state estimator are

$$\dot{\hat{\bar{\chi}}} = A_{\text{aug}}\hat{\bar{\chi}} + B_1\bar{u}_p + M_1\left(\bar{y}_p - C_{\text{aug}}\hat{\bar{\chi}}\right) \tag{A18}$$

where the Kalman filter gain matrix M_1 is given by

$$M_1 = \Sigma C_{\text{aug}}^TV_y^{-1} \tag{A19}$$

with $\Sigma(\geq 0)$ the solution of the algebraic Ricatti equation

$$A_{\text{aug}}\Sigma + \Sigma A_{\text{aug}}^T + DWD^T - \Sigma C_{\text{aug}}^TV_y^{-1}C_{\text{aug}}\Sigma = 0 \tag{A20}$$

Solution for $\bar{u}_a$ and $\bar{u}_d$

The optimal controller $\bar{u}_p$, as derived above, has the form

$$\bar{u}_p = K_p\hat{\bar{\chi}}, \quad \dot{\hat{\bar{\chi}}} = A_1\hat{\bar{\chi}} + M_1\bar{y}_p \tag{A21}$$

where $A_1 \triangleq (A_{\text{aug}} + B_1K_p - M_1C_{\text{aug}})$. Then, in the presence of this control action $\bar{u}_p$, the system dynamics [Eqs. (A9), (A15), and (A18)] can be written in terms of the augmented state vector $\bar{q} \triangleq \text{col}(\bar{\chi}, \hat{\bar{\chi}})$ as

$$\dot{\bar{q}} = \begin{bmatrix} A & B_1K_p \\ M_1C_1 & A_1 \end{bmatrix}\bar{q} + \begin{bmatrix} B_2 \\ 0 \end{bmatrix}\bar{u}_a + \begin{bmatrix} B_d \\ M_1C_u \end{bmatrix}\bar{u}_d + \begin{bmatrix} D & 0 \\ 0 & M_1 \end{bmatrix}\begin{Bmatrix} \bar{w} \\ \bar{v}_y \end{Bmatrix} \tag{A22}$$

which can be written in a compact form, with appropriate definitions of matrices, as

$$\dot{\bar{q}} = A_1'\bar{q} + B_2'\bar{u}_a + B_d'\bar{u}_d + D'\bar{w}' \tag{A23}$$

The intensity of the process $\bar{w}'$ is $W' = \begin{bmatrix} W & 0 \\ 0 & V_y \end{bmatrix}$.

The index of performance to be minimized by $\bar{u}_a$ and $\bar{u}_d$ then becomes

$$J_2 = E\left\{ \lim_{T\to\infty} \frac{1}{T}\int_o^T \left(\bar{q}^TQ'\bar{q} + \bar{u}_a^TF_2\bar{u}_a + \bar{u}_d^TF_{2d}\bar{u}_d\right) \mathrm{d}t \right\} \tag{A24}$$

with

$$Q' \triangleq \begin{bmatrix} Q_2 & 0 \\ 0 & K_p^TR_2K_p \end{bmatrix}$$

The design objective can then be stated as that of finding the optimal controller $\bar{u}_a$ and optimal display control $\bar{u}_d$, which minimize the cost J_2 as given by Eq. (A24), subject to Eq. (A23).

It can be shown[22] that the gains G_a and G_d, which correspond to the simultaneous optimality of the two controllers $\bar{u}_a$ and $\bar{u}_d$, are given by

$$G_a = -F_2^{-1}\begin{bmatrix} B_2^T & 0 \end{bmatrix} HL\begin{bmatrix} C_2^T \\ 0 \end{bmatrix}\left(\begin{bmatrix} C_2 & 0 \end{bmatrix} L\begin{bmatrix} C_2^T \\ 0 \end{bmatrix}\right)^{-1} \tag{A25}$$

and

$$G_d = -F_{2d}^{-1}\begin{bmatrix} B_d \\ M_1C_u \end{bmatrix}^T HL\begin{bmatrix} C_d^T \\ 0 \end{bmatrix}\left(\begin{bmatrix} C_d & 0 \end{bmatrix} L\begin{bmatrix} C_d^T \\ 0 \end{bmatrix}\right)^{-1} \tag{A26}$$

Here, $L = E\{\bar{q}\bar{q}^T\}$ satisfies the relation

$$A_cL + LA_c^T + D'W'D'^T = 0 \tag{A27}$$

and H satisfies

$$A_c^TH + HA_c + \bar{Q} = 0 \tag{A28}$$

where the following definitions have been used

$$A_c \triangleq \begin{bmatrix} A_{\text{aug}} & B_1K_p \\ M_1C_{\text{aug}} & A_1 \end{bmatrix};$$
$$\bar{Q} \triangleq Q' + \begin{bmatrix} C_2^TG_a^TF_2G_aC_2 + C_d^TG_d^TF_{2d}G_dC_d & 0 \\ 0 & 0 \end{bmatrix}$$

The solutions (A25) and (A26) are derived from the gradient conditions

$$\frac{\partial \bar{J}_2}{\partial G_a} = 2\left\{ F_2G_a\begin{bmatrix} C_2 & 0 \end{bmatrix} L\begin{bmatrix} C_2^T \\ 0 \end{bmatrix} + \begin{bmatrix} B_2^T & 0 \end{bmatrix} HL\begin{bmatrix} C_2^T \\ 0 \end{bmatrix}\right\} = 0 \tag{A29}$$

$$\frac{\partial \bar{J}_2}{\partial G_d} = 2\left\{ F_{2d}G_d\begin{bmatrix} C_d & 0 \end{bmatrix} L\begin{bmatrix} C_d^T \\ 0 \end{bmatrix} + \begin{bmatrix} B_d \\ M_1C_u \end{bmatrix}^T HL\begin{bmatrix} C_d^T \\ 0 \end{bmatrix}\right\} = 0 \tag{A30}$$

respectively.

Thus, the solution to the cooperative control/display synthesis problem requires simultaneously solving two algebraic Ricatti equations [Eq. (A17) for the control gains for controller 1 ($\bar{u}_p$) and Eq. (A20) for the estimator gains], two

Lyapunov equations [Eq. (A27) for the system covariance matrix and Eq. (A28) for the matrix of Lagrange multipliers], and two gradient conditions [Eqs. (A29) and (A30)] that are necessary for the optimality of the gains G_a and G_d. A computer program using a conjugate gradient search algorithm with cubic interpolation[23] was developed to solve for the optimal augmentation gains.

Acknowledgment

This research was supported by NASA Dryden Flight Research Facility, Ames Research Center, under Grants NAG2-228 and NAG4-1. Mr. E.L. Duke and Mr. Donald T. Berry are the technical monitors. This support is gratefully appreciated.

References

[1]"V/STOL Displays for Approach and Landing," Advisory Group for Aerospace Research and Development Rept. No. 594, 1972.

[2]Lebacqz, J.V., Gerdes, R.M., Forrest, R.D., and Merrill, R.K., "Investigation of Control, Display, and Crew-Loading Requirements for Helicopter Instrument Approach," *Journal of Guidance and Control*, Vol. 4, Nov.–Dec. 1981, pp. 614–622.

[3]Lebacqz, J.V., "Ground Simulation Investigation of Helicopter Decelerating Instrument Approaches," *Journal of Guidance and Control*, Vol. 6, Sept.–Oct. 1983, pp. 330–338.

[4]Duke, E.L., Jones, F.P., and Roncoli, R.B., "Development of a Flight Test Maneuver Autopilot for a Highly Maneuverable Aircraft," AIAA Paper 83-0061, Jan. 1983.

[5]Duke, E.L., Swann, M.R., Enevoldson, E.K., and Wolf, T.D., "Experience with Flight Test Trajectory Guidance," *Journal of Guidance and Control*, Vol. 6, Sept.–Oct. 1983, pp. 393–398.

[6]Schmidt, D.K., "Optimal Flight Control Synthesis via Pilot Modeling," *Journal of Guidance and Control*, Vol. 2, July–Aug. 1979, pp. 308–312.

[7]Kleinman, D.L., Baron, S., and Levison, W.H., "An Optimal Control Model of Human Response," Parts I and II, *Automatica*, Vol. 6, May 1970, pp. 357–383.

[8]Levison, W.H., "A Model Based Technique for the Design of Flight Directors," *Proceedings of the Ninth Annual Conference on Manual Control*, NASA CR-142295, May 1973, pp. 163–172.

[9]Hess, R.A., "Analytical Display Design for Flight Tasks Conducted Under Instrument Meteorological Conditions," NASA TMX-73,146, Aug. 1976.

[10]Hoffman, W.C., Kleinman, D.L., and Young, L.R., "Display/Control Requirements for Automated VTOL Aircraft," NASA CR-158905, ASI-TR-76-39, Oct. 1976.

[11]Weir, D.H., Klein, R.H., and McRuer, D.T., "Principles for the Design of Advanced Flight Director Systems Based on the Theory of Manual Control Displays," NASA CR-1748, March 1971.

[12]McRuer, D.T. and Jex, H.R., "A Review of QuasiLinear Pilot Models," *Transactions of Human Factors in Electronics*, Vol. HFE-8, No. 3, Sept. 1967, pp. 231–249.

[13]Schmidt, D.K. and Innocenti, M., "Optimal Cooperative Control Applied to a Control Configured Aircraft," NASA CR-170411, Jan. 1984.

[14]Phatak, Anil V., "Investigation of Alternate Human Operator Optimal Control Structures," Aerospace Medical Research Labs, Wright-Patterson AFB, OH, Contract F33615-78-C-0501, 1978.

[15]Wierwille, W.W. and Connor, S.A., "Evaluation of 20 Workload Measures Using a Psychomotor Task in a Moving-Base Aircraft Simulator," *Human Factors*, Vol. 25, 1983, pp. 1–16.

[16]Schmidt, D.K., "On the Use of the OCM's Objective Function as a Pilot Rating Metric," *Proceedings of 17th Annual Conference on Manual Control*, NASA CR-165005, June 1981, pp. 305–313.

[17]Bacon, B.J. and Schmidt, D.K., "An Optimal Control Approach to Pilot/Vehicle Analysis and the Neal-Smith Criteria," *Journal of Guidance and Control*, Vol. 6, Sept.–Oct. 1983, pp. 339–347.

[18]McDonnell, J.D., "Pilot Rating Techniques for the Estimation and Evaluation of Handling Qualities," Air Force Flight Dynamics Laboratory, Wright-Patterson AFB, OH, TR-68-76, Dec. 1968.

[19]Cooper, G.E., "Understanding and Interpreting Pilot Opinion," *Aeronautical Engineering Review*, Vol. 16, No. 3, Mar. 1957, pp. 47–52.

[20]Pavassilopoulos, G.P., Medanic, J.V., and Cruz, J.B. Jr., "On the Existence of Nash Strategies and Solutions to Coupled Ricatti Equations in Linear-Quadratic Games," *Journal of Optimization Theory and Applications*, Vol. 28, No. 1, May 1979, pp. 49–76.

[21]Kwakernaak, H. and Sivan, R., *Linear Optimal Control Systems*, Wiley-Interscience, New York, 1972.

[22]Garg, S. and Schmidt, D.K., "Optimal Cooperative Control Synthesis of Active Displays," NASA CR-4058, June 1987.

[23]Fletcher, R. and Powell, M.J.D., "A Rapidly Convergent Descent Method for Minimization," *Computer Journal*, Vol. 6, July 1963, pp. 163–168.